

A BENCHMARK CALCULATION OF 3D HORIZONTAL WELL SIMULATIONS

ZHANGXIN CHEN, GUANREN HUAN, AND BAOYAN LI

Abstract. The simulation of realistic multiphase flow problems in petroleum reservoirs requires means for handling the complicated structure of the reservoirs such as complex boundaries, faults, fractures, and horizontal wells. A numerical reservoir simulator has recently been developed to be able to handle these features for a wide range of applications. This fully implicit simulator is based on a three-dimensional, three-phase black oil model. It can also be used to solve a dual-porosity, dual-permeability black oil model in a fractured reservoir. The space discretization method used in this simulator is based on a block-centered finite difference method with harmonic averaged coefficients (equivalently, a mixed finite element method). In this paper we report an application of this simulator to a problem involving injection and production from horizontal wells in a reservoir where a coning tendency is important, and present a benchmark comparison with other simulators by fourteen petroleum organizations.

Key Words. reservoir simulator, black oil model, horizontal well, block-centered finite difference, mixed finite element, numerical experiments.

1. Introduction

Because of improved drilling technology interest in the modeling and numerical simulation of horizontal wells in petroleum reservoirs has been rapidly increased [3]. The use of horizontal wells not only leads to the increased efficiency and economy of oil recovery operations, also it decreases the coning behavior with an increase in well length and enlarges oil sweeping volumes. For gas reservoirs with low permeability, it decreases turbulence effects at gas wells and increases production rates.

This paper studies a problem which is concerned with the effect of horizontal well lengths and rates on oil recovery. This effect is studied using a reservoir simulator we have recently developed. This simulator is fully implicit and is based on a three-dimensional, three-phase black oil model. It is capable of handling a fractured reservoir with dual-porosity and dual-permeability. It can model nonlinear flow around gas wells, treat some highly volatile oil and gas condensate systems, and implement complex reservoir depletion projects. The space discretization method used in this simulator is based on a block-centered finite difference method with harmonic averaged coefficients (equivalently, a mixed finite element method [5]).

In this paper we report an application of our simulator to a problem involving injection and production from horizontal wells in a reservoir where a coning tendency is important, and present a benchmark comparison with other simulators by fourteen petroleum organizations. The comparison is on oil production rates, water-oil

Received by the editors February 3, 2004.

2000 *Mathematics Subject Classification.* 35K60, 35K65, 76S05, 76T05.

production ratios, and pressures. This comparison indicates that our results are close to the mean values of those by these fourteen organizations' simulators, which shows the correctness and reliability of our simulator. After we are confident with our simulator, we use it to test well lengths and rates on oil recovery. This test predicts an increase in oil production and a decrease in coning effects with an increase in well length. We also present a benchmark comparison between the compressible case and the incompressible case for the black oil model considered. This comparison surprisingly shows that the numerical results match very well in these two cases for the present model, and thus the incompressible case is a quite reasonable approximation of the compressible case. This experiment provides a sound numerical basis for the common practice where the incompressible case is usually employed for reservoir simulation tests because of its simple implementation.

This paper is outlined in the following fashion. In the next section we review a three-dimensional, three-phase black oil model. Then, in the third section we introduce the physical data for our numerical tests. The comparisons are carried out in the fourth and fifth sections. Concluding remarks are given in the last section.

2. A Black Oil Model

In the black oil model problem considered, it is assumed that there are at most three distinct phases: gas, oil, and water. Usually water is the wetting phase, oil has an intermediate wettability, and gas is the nonwetting phase. Water and oil are assumed to be immiscible and they do not exchange mass. Gas is assumed to be soluble in oil but usually not in water. If the solubility of gas is assumed to be zero at stock tank conditions, then reservoir oil can be considered to be a solution of two components: stock tank oil and gas at standard conditions. Furthermore, in this kind of treatment it is assumed that the fluids are at constant temperature and in thermodynamic equilibrium throughout a reservoir. Under these conditions the model equations for mass balance are given by [1]

$$\begin{aligned}\frac{\partial}{\partial t}(\phi\rho_w s_w) + \nabla \cdot (\rho_w \mathbf{u}_w) &= \rho_w q_w, \\ \frac{\partial}{\partial t}(\phi\rho_o^o s_o) + \nabla \cdot (\rho_o^o \mathbf{u}_o) &= \rho_o^o q_o, \\ \frac{\partial}{\partial t}(\phi[\rho_o^g s_o + \rho_g s_g]) + \nabla \cdot (\rho_o^g \mathbf{u}_o + \rho_g \mathbf{u}_g) &= \rho_o^g q_o^g + \rho_g q_g,\end{aligned}$$

where the subscripts w , o , and g stand for water, oil, and gas, respectively, ϕ is the porosity of the reservoir, ρ_α , s_α , and \mathbf{u}_α are the density, saturation, and volumetric velocity of the α -phase, $\alpha = w, o, g$, and q_w , q_o , q_o^g , and q_g denote source/sink terms. The density ρ_o of the oil phase is

$$\rho_o = \rho_o^o + \rho_o^g,$$

where ρ_o^o and ρ_o^g indicate the partial densities of the two components in the oil phase. The phase densities at reservoir conditions are related to densities at stock tank conditions ($\bar{\rho}_w$, $\bar{\rho}_o$, and $\bar{\rho}_g$) as follows:

$$\rho_w = \frac{\bar{\rho}_w}{B_w}, \quad \rho_o = \frac{\bar{\rho}_o + R_s \bar{\rho}_g}{B_o}, \quad \rho_g = \frac{\bar{\rho}_g}{B_g},$$

where B_α is the formation volume factor of the α -phase, $\alpha = w, o, g$, and R_s is the gas solubility. Note that

$$\rho_o^o = \frac{\bar{\rho}_o}{B_o}, \quad \rho_o^g = \frac{R_s \bar{\rho}_g}{B_o}.$$

The volumetric velocity \mathbf{u}_α is given by Darcy's law

$$\mathbf{u}_\alpha = -\frac{K_{r\alpha}}{\mu_\alpha} \mathbf{K}(\nabla p_\alpha - \rho_\alpha \tilde{g} \nabla Z), \quad \alpha = w, o, g,$$

where \mathbf{K} is the absolute permeability of the reservoir, p_α , μ_α , and $K_{r\alpha}$ are the pressure, viscosity, and relative permeability of the α -phase, respectively, \tilde{g} denotes the gravitational constant, and Z is the depth. The pressures are related by the capillary pressure functions

$$p_{cw} = p_o - p_w, \quad p_{cg} = p_g - p_o.$$

Finally, the saturations satisfy

$$s_w + s_o + s_g = 1.$$

The densities, viscosities, gas solubility, and formation volume factors are functions of pressures, and the capillary pressures and relative permeabilities are functions of saturations. Hence these model equations are strongly nonlinear for the unknowns p_α , \mathbf{u}_α , and s_α . They can be reformulated in different forms with three main unknowns (e.g., a pressure and two saturations) [2]. In the case where all gas dissolves into oil, the three-phase system becomes a two-phase system where the gas phase disappears. In this case, oil is said to be under-saturated. While we just state the case where gas dissolves into oil in the black oil model, our simulator can also treat other cases such as the case where oil volatilizes into gas, as noted.

We conclude this section with the definition of source/sink terms. Following [4], q_w at a well can be defined by

$$q_w = PI \frac{K_{rw}}{\mu_w} (p_{BH} - p_w - \rho_w \tilde{g} (Z_{BH} - Z)),$$

where PI is the productivity index of this well and p_{BH} is the flowing bottom hole pressure at the datum level depth Z_{BH} . Similarly, we define

$$\begin{aligned} q_o^o &= q_o^g = PI \frac{K_{ro}}{\mu_o} (p_{BH} - p_o - \rho_o \tilde{g} (Z_{BH} - Z)), \\ q_g &= PI \frac{K_{rg}}{\mu_g} (p_{BH} - p_g - \rho_g \tilde{g} (Z_{BH} - Z)). \end{aligned}$$

The productivity index PI is given by

$$PI = 2\pi \bar{K} h / \ln \frac{r_e}{r_c},$$

where the quantity \bar{K} is some average of \mathbf{K} at a well, h is the depth of the well, r_e is the equivalent radius, and r_c is the radius of the well. For a diagonal tensor $\mathbf{K} = \text{diag}(K_{11}, K_{11}, K_{33})$ and a vertical well, for example, \bar{K} and r_e are defined as

$$\bar{K} = K_{11}, \quad r_e = 0.14 (DX^2 + DY^2)^{1/2},$$

where K_{11} and K_{33} are the permeabilities in the horizontal and vertical directions, respectively, and DX and DY are the x - and y -dimensions of the grid block which contains this vertical well. For a diagonal tensor \mathbf{K} and a horizontal well (e.g., in the x -direction), \bar{K} and r_e are determined by

$$\bar{K} = \sqrt{K_{11} K_{33}}, \quad r_e = \frac{0.14 \left(\left(\frac{K_{33}}{K_{11}} \right)^{1/2} DX^2 + \left(\frac{K_{11}}{K_{33}} \right)^{1/2} DY^2 \right)^{1/2}}{0.5 \left(\left(\frac{K_{33}}{K_{11}} \right)^{1/4} + \left(\frac{K_{11}}{K_{33}} \right)^{1/4} \right)},$$

where DZ is the z -dimension of the grid block containing this horizontal well.

3. Physical Data

The physical data for a reservoir and fluids are taken from [3] for a benchmark three-dimensional, three-phase black oil problem and are given in Tables 1–3 and 5 where s.c. stands for standard condition. The first Stone three-phase relative-permeability model [6] is used. For the present problem, the use of the second Stone model generates similar results because very little free gas is produced.

The problem considered deals with oil recovery by bottom water drive in a reservoir where coning is important. Fluids are produced from a horizontal well drilled in the top layer (Layer one). This well passes through the grid block centers and the entire length is open to flow. Two lengths are presented: (a) $L = 900$ ft and the well is stretched in grid blocks $(i, 5, 1)$, $i = 6, 7, 8$; (b) $L = 2, 100$ ft and the well is stretched in grid blocks $(i, 5, 1)$, $i = 2, 3, \dots, 8$. The flow direction in this well is from left to right, and the fluids are removed from the portion of this well in grid block $(8, 5, 1)$ to the surface.

A constant pressure line source is exploited to simulate the bottom water drive. This line source is stretched in grid blocks $(i, 5, 6)$, $i = 1, 3, \dots, 9$. The horizontal production well produces at a constant liquid (water and oil) rate. Three rates are presented and a total number of six cases are considered:

- case 1a : $L = 900$ ft and the liquid rate is 3,000 stb/day,
- case 1b : the same as case 1a but with $L = 2, 100$ ft,
- case 2a : $L = 900$ ft and the liquid rate is 6,000 stb/day,
- case 2b : the same as case 2a but with $L = 2, 100$ ft,
- case 3a : $L = 900$ ft and the liquid rate is 9,000 stb/day,
- case 3b : the same as case 3a but with $L = 2, 100$ ft.

s_w	0.22	0.3	0.4	0.5	0.6	0.8	0.9	1
K_{rw}	0	0.07	0.15	0.24	0.33	0.65	0.83	1
K_{row}	1	0.4	0.125	0.0649	0.0048	0	0	0
p_{cw}	6.3	3.6	2.7	2.25	1.8	0.9	0.45	0.0

Table 1. The relative permeabilities and capillary pressure for water/oil system.

s_g	0.0	0.04	0.1	0.2	0.3	0.4	0.5	0.6	0.7	0.78
K_{rg}	0.0	0.0	0.022	0.1	0.24	0.34	0.42	0.5	0.8125	1.0
K_{rog}	1.0	0.6	0.33	0.1	0.02	0	0	0	0	0
p_{cw}	0.0	0.2	0.5	1.0	1.5	2.0	2.5	3.0	3.5	3.9

Table 2. The relative permeabilities and capillary pressure for gas/oil system.

p (psia)	R_s (scf/stb)	μ_o (cp)	B_o (rb/stb)	μ_g (cp)	B_g (rb/scf)
400	165	1.17	1.012	0.0130	0.0059
800	335	1.14	1.0255	0.0135	0.00295
1,200	500	1.11	1.038	0.0140	0.00196
1,600	665	1.08	1.051	0.0145	0.00147
2,000	828	1.06	1.063	0.0150	0.00118
2,400	985	1.03	1.075	0.0155	0.00098
2,800	1,130	1.00	1.087	0.0160	0.00084
3,200	1,270	0.98	1.0985	0.0165	0.00074
3,600	1,390	0.95	1.11	0.0170	0.00065
4,000	1,500	0.94	1.12	0.0175	0.00059
4,400	1,600	0.92	1.13	0.0180	0.00054
4,800	1,676	0.91	1.14	0.0185	0.00049
5,200	1,750	0.90	1.148	0.0190	0.00045
5,600	1,810	0.89	1.155	0.0195	0.00042

Table 3. The oil and gas PVT table.

Participant	1a	1b	2a	2b	3a	3b
ARTEP	747.2	951.7	976.4	1221.0	1096.4	1318.5
Chevron	741.0	929.4	958.1	1181.6	1066.0	1274.8
CMG	753.6	960.1	983.6	1230.3	1106.1	1330.2
ECL	757.2	951.0	1034.2	1251.0	1229.1	1444.8
ERC	683.5	870.2	900.3	1106.1	1031.4	1222.3
HOT	765.0	961.9	1045.9	1263.7	1247.0	1466.8
INTECH	723.3	957.5	949.6	1241.5	1103.2	1414.7
JNOC	717.4	951.3	931.6	1245.9	1084.4	1412.7
Marathon	722.9	964.3	941.5	1257.1	1096.0	1436.7
Phillip's	750.9	956.8	980.5	1227.1	1103.5	1325.0
RSRC	678.7	916.7	877.9	1177.8	1017.1	1333.2
Shell	749.0	954.8	978.4	1224.6	1100.0	1322.4
Stanford	742.0	943.9	968.7	1211.8	1043.7	1305.6
TDC	766.2	980.4	989.4	1210.0	1105.0	1279.2
Max	766.2	980.4	1045.9	1257.1	1247.0	1466.8
Mean	735.6	946.4	965.4	1217.8	1102.1	1349.1
Min	678.7	870.2	877.9	1106.1	1017.1	1222.3
SMU	709.0	932.5	929.2	1214.7	1079.8	1380.7

Table 4. The cumulative oil production comparison.

Item	Unit	Data
Dimensions $NX \times NY \times NZ$		$9 \times 9 \times 6$
Grid size DX	ft	$9 * 300$
Grid size DY	ft	620 400 200 100 60 100 200 400 620
Grid size DZ	ft	20 20 20 20 30 50
Depth of grid centers in z	ft	3600 3620 3640 3660 3685 3725
Initial water saturation in z	frac	0.289 0.348 0.473 0.649 0.869 1.00
Porosity	frac	0.2
Horizontal permeability	md	300
Vertical permeability	md	30
Rock compressibility	1/psi	$4E - 6$
Reference pressure	psia	3600
Water density at s.c.	lbm/ft ³	62.14
Water viscosity	cp	0.96
Water formation factor	rb/stb	1.0142
Water compressibility	1/psi	$3E - 6$
Oil density at s.c.	lbm/ft ³	45
Oil viscosity compressibility	1/psi	0
Oil compressibility	1/psi	$1E - 5$
Gas density at s.c.	lbm/ft ³	0.0702
Radius of wellbore	inches	2.25
Time step for calculation	days	100
Ultimate time for calculation	days	1,500
Length of oil horizontal well	ft	900 (for cases 1a, 2a, 3a)
Length of oil horizontal well	ft	2,100 (for cases 1b, 2b, 3b)
Length of water horizontal well	ft	2,700 (for all cases)
Layer of oil horizontal well		1
Layer of water horizontal well		6
Grids of horizontal wells in y		5 (for all cases)
Grids of oil well in x		6-8 (for cases 1a, 2a, 3a)
Grids of oil well in x		2-8 (for cases 1b, 2b, 3b)
Min. bottom hole pressure of oil	psia	1,500
Liquid production rate	stb/day	3,000 (for cases 1a, 1b)
Liquid production rate	stb/day	6,000 (for cases 2a, 2b)
Liquid production rate	stb/day	9,000 (for cases 3a, 3b)

Table 5. The physical and fluid data.

4. Comparison I

The six cases presented in the previous section examine the effect of rates and well lengths on oil recovery. Since the pressure at the injection well is fixed, very little free gas is produced, as mentioned. In this section we present a comparison of our reservoir simulator for the present benchmark problem with other simulators by fourteen petroleum organizations. The comparison is on daily oil production rates, cumulative oil production, water-oil production ratios, and bottom hole pressures at the producer. As noted, our simulator solves all coupled differential equations simultaneously (i.e., fully implicit) and uses a block-centered finite difference method with harmonic averaged coefficients (equivalently, a mixed finite element method) as

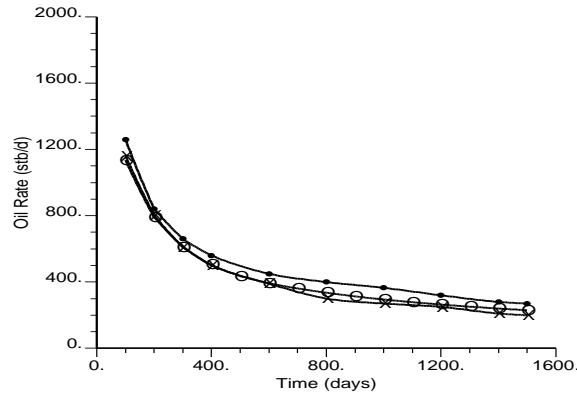
the space discretization method. It employs a Newton-Raphson solution algorithm which, due to fewer iterations per time step, is very efficient for large nonlinear equations, and a linear solver is based on a preconditioned Orthomin iterative procedure. This iterative procedure is very efficient for the solution of nonsymmetric linear systems of algebraic equations.

The fourteen organizations involved are ARTEP (Research Association of Institut Francais du Pétrole), Chevron (Chevron Oil Field Research Company), CMG (Computer Modeling Group), ECL (ECL Petroleum Technologies), ERC (Robertson ERC Limited), HOT (HOT Engineering), INTECH (Integrated Technologies), JNOC (Japan National Oil Corporation), Marathon (Marathon Oil Company), Phillip's (Phillip's Petroleum Company), RSRC (Reservoir Simulation Research Corporation), Shell (Shell Development Company), Stanford (Stanford University), and TDC (TDC Reservoir Engineering Services). Our simulator is termed SMU (Southern Methodist University). The space discretization method in these fourteen organizations is based on the finite difference method, and most of them model horizontal wells in the same approach as ours.

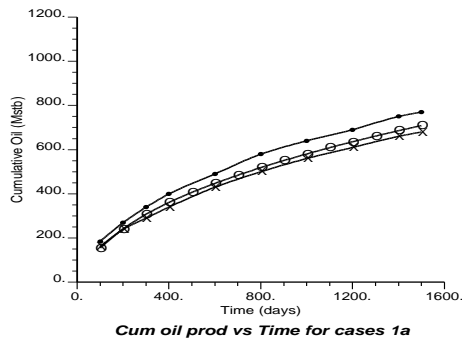
Participant	1a	1b	2a	2b	3a	3b
ARTEP	3466.76	3575.78	3236.68	3470.49	3002.20	3364.74
Chevron	3464.77	3576.10	3239.19	3464.32	3012.13	3356.08
CMG	3446.32	3558.33	3210.46	3454.76	2970.39	3345.85
ECL	3485.03	3569.71	3326.22	3490.41	3170.46	3412.53
ERC	3439.96	3562.14	3199.89	3453.11	2949.06	3343.41
HOT	3511.65	3582.92	3382.08	3520.19	3256.18	3459.89
INTECH	3530.00	3601.00	3382.00	3541.00	3221.00	3479.00
JNOC	3471.72	3589.29	3251.86	3491.07	3020.84	3405.28
Marathon	3493.24	3593.85	3295.26	3509.80	3085.07	3433.56
Phillip's	3449.40	3572.40	3203.40	3460.20	2953.20	3351.90
RSRC	3567.80	3610.90	3444.10	3575.30	3318.90	3530.30
Shell	3448.75	3571.38	3201.16	3456.91	2948.98	3345.16
Stanford	3454.64	3572.29	3216.69	3464.30	2977.69	3359.93
TDC	3438.21	3544.40	3203.95	3452.69	2959.82	3343.16
Max	3567.80	3610.90	3444.10	3575.30	3318.90	3530.30
Mean	3476.30	3577.18	3270.92	3486.04	3060.42	3395.06
Min	3438.21	3544.40	3199.89	3454.76	2948.98	3343.41
SMU	3463.55	3586.66	3230.98	3484.47	2991.40	3393.62

Table 6. The bottom hole pressure comparison at the producer.

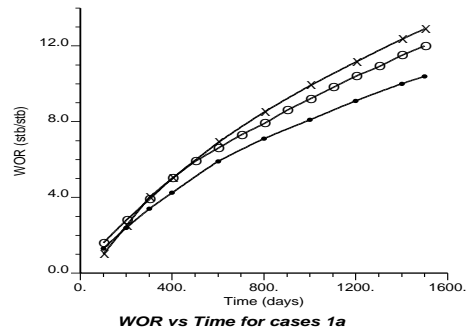
The cumulative oil production (in mstb) at 1,500 days by the fourteen organizations and SMU is shown in Table 4, and the bottom hole pressure (in psia) comparison at the producer is presented in Table 6. These two tables indicate that our results are close to the mean values of those by these organizations, which shows the correctness and reliability of our simulator. This can also be seen from Figs. 1-3 where the maximum and minimum values of the daily oil production rates (stb/days), cumulative oil production, and water-oil ratios (WOR, stb/stb) verse time for case 1a by these fourteen organizations and the corresponding results by our simulator are displayed, respectively.



Oil Rate vs Time for cases 1a
 Fig. 1: ●=max, ×=min, ○=SMU.



Cum oil prod vs Time for cases 1a
 Fig. 2: ●=max, ×=min, ○=SMU.



WOR vs Time for cases 1a
 Fig. 3: ●=max, ×=min, ○=SMU.

After we get confidence with our simulator from the above comparison, we now use it to compare the six cases considered. The daily oil production rates between cases 1a, 2a, and 3a and between cases 1b, 2b, and 3b are displayed, respectively, in Figs. 4 and 5. The corresponding comparisons for the cumulative oil production and water-oil ratios are shown in Figs. 6–9. Also, the comparisons for these quantities between cases 1a and 1b are presented in Figs. 10–12. From these figures, we summarize the following observations:

- Oil production increases as the well length increases, but the production increase is limited and is not directly proportional to the length. As an example, from the comparison between cases 1a and 1b, we see that the well length of 1b is over two times longer than that of 1a, but the cumulative oil production at 1,500 days increases only 31.5% (see Figs. 10 and 11).

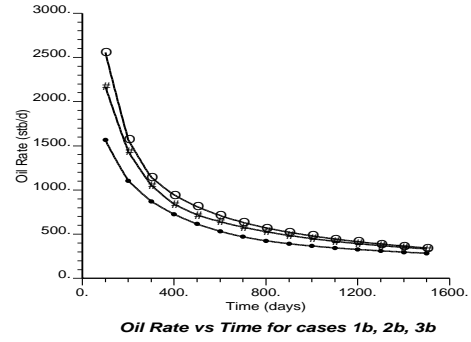
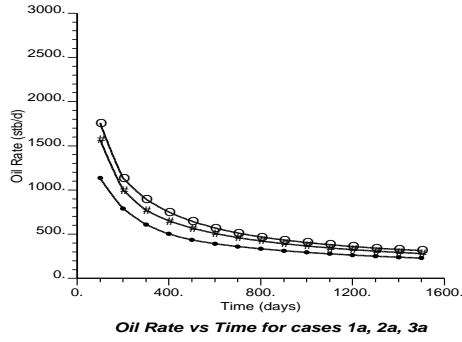


Fig. 4: ●=1a, #=2a, and ○=3a.

Fig. 5: ●=1b, #=2b, and ○=3b.

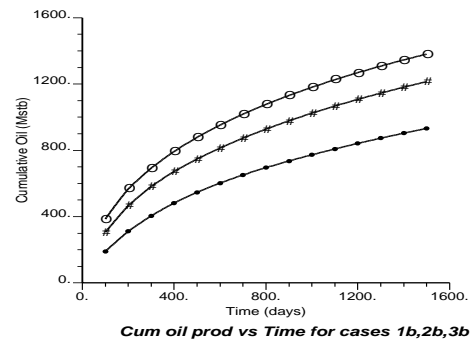
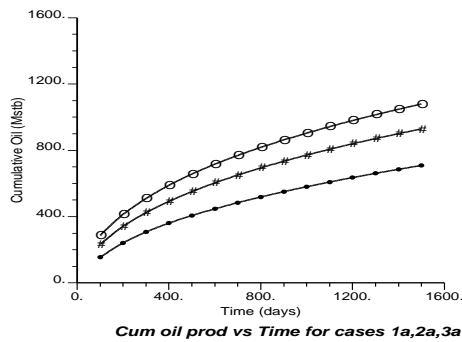


Fig. 6: ●=1a, #=2a, and ○=3a.

Fig. 7: ●=1b, #=2b, and ○=3b.

- The water coning effect decreases as the well length increases. Although the production rate in case 1b is higher than in case 1a, for example, the water-oil ratio in 1b is lower than in 1a (see Fig. 12). This implies that the well length increase overcomes the effect of water coning. This phenomenon can be seen also from Figs. 8 and 9, where this ratio is lower in all cases 1b, 2b, and 3b.
- For the horizontal well, oil production increases as liquid (water and oil) production increases, but the effect of water coning also increases at the same time. In turn, part of the coning effect offsets the role of increasing liquid production. Comparing case 3a with case 1a, and case 3b with case 1b, for example, the liquid production is three times more, but the cumulative oil production at 1,500 days increases only 52.3% and 48.1%, respectively. This indicates that as liquid production increases, pressure

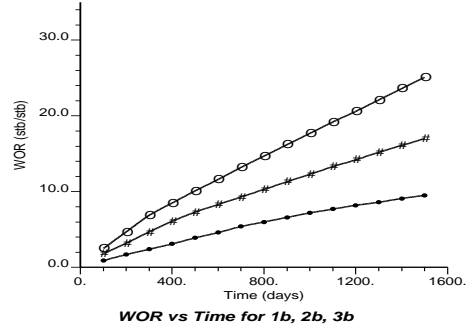
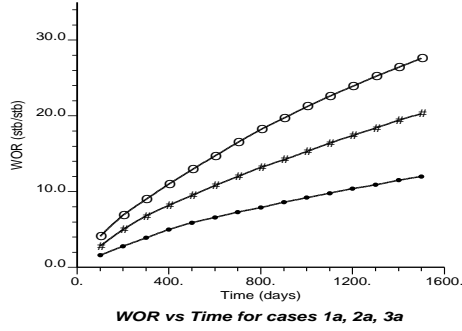


Fig. 8: ●=1a, #=2a, and ○=3a. Fig. 9: ●=1b, #=2b, and ○=3b.

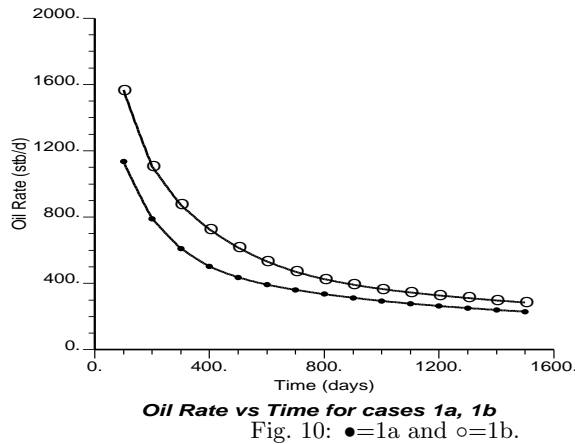


Fig. 10: ●=1a and ○=1b.

drop enlarges, the gravity effect decreases, and the coning effect strengthens. All these lead to a high water-oil ratio (see Figs. 8 and 9). This is why the oil production suddenly decreases at the early stages of the highest liquid production cases 3a and 3b (see Figs. 4 and 5).

- For the purpose of increasing oil production, increasing the well length is better than increasing the liquid production.

5. Comparison II

In this section we consider the oil under-saturated case where the three-phase system becomes a two-phase system, i.e., the gas phase totally disappears. Furthermore, we assume that the water and oil compressibilities are zero. That is, we

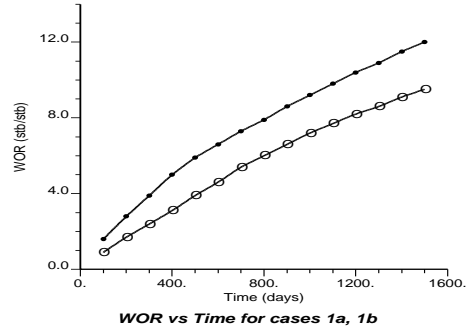
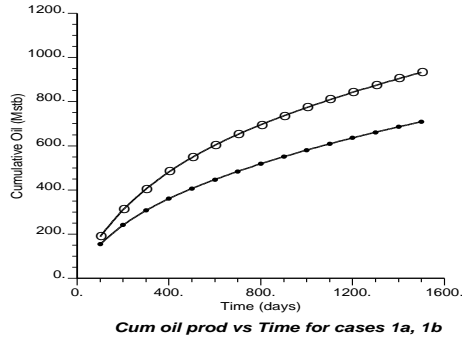


Fig. 11: ●=1a and ○=1b. Fig. 12: ●=1a and ○=1b.

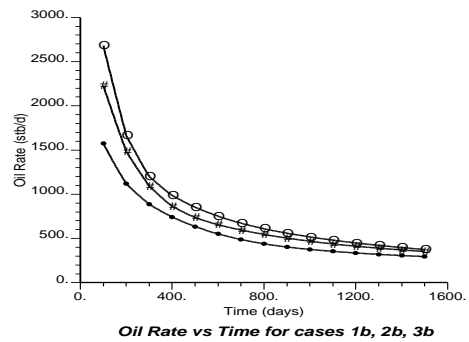
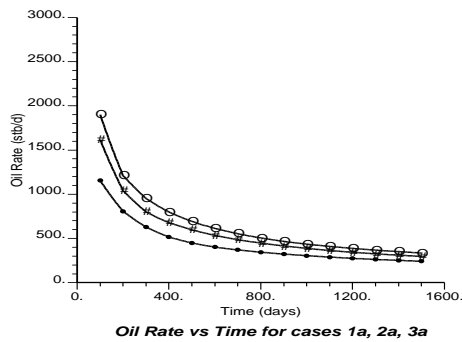


Fig. 13: ●=1a, #=2a, and ○=3a. Fig. 14: ●=1b, #=2b, and ○=3b.

consider two-phase incompressible flow in this section. The rock compressibility is also assumed to be zero. All other physical data are the same as in the previous two sections.

The cumulative oil production at 1,500 days obtained using our simulator for the compressible and incompressible cases is shown in Table 7, and the bottom hole pressure comparison at the producer is given in Table 8. From these tables we see that the incompressible case is a quite reasonable approximation of the compressible case. In fact, the bottom hole pressures obtained in the incompressible case can be used as a fixed pressure condition at production wells for the compressible case, instead of using a constant liquid rate condition. This will simplify the computation of the compressible case. The daily oil production rates, cumulative oil production, and water-oil ratios verse time for the incompressible case are shown in Figs. 13–18. The observations made in the previous section on the well lengths, liquid production

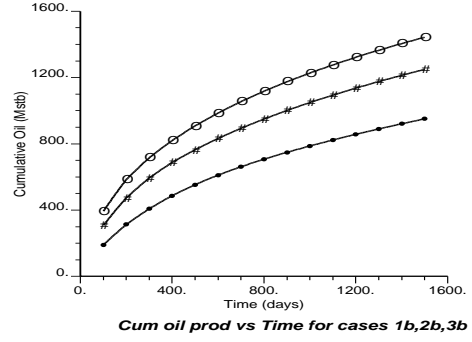
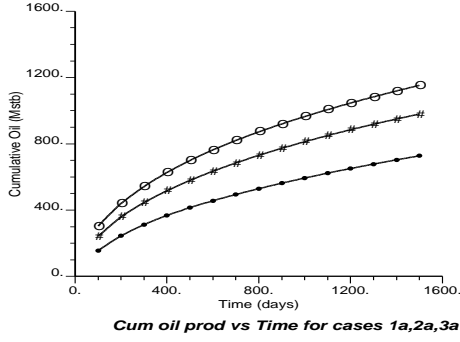


Fig. 15: ●=1a, #=2a, and ○=3a.

Fig. 16: ●=1b, #=2b, and ○=3b.

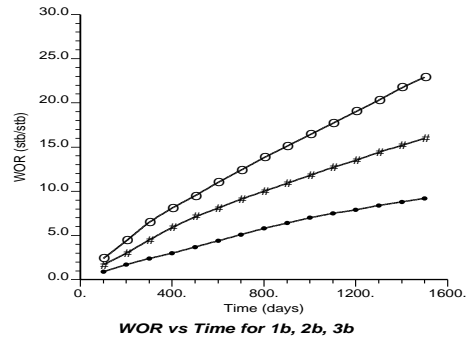
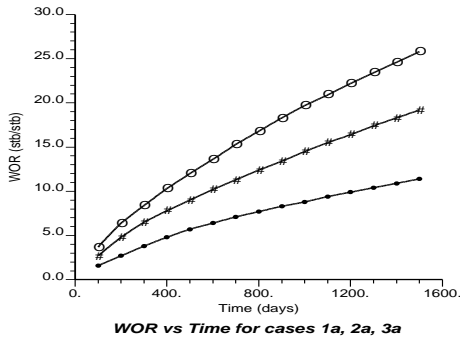


Fig. 17: ●=1a, #=2a, and ○=3a.

Fig. 18: ●=1b, #=2b, and ○=3b.

rates, and coning effects also apply to the present case. Therefore, we can just use the incompressible case to study the effect of horizontal well lengths and rates on oil recovery. This significantly simplifies all computations. The present experiment provides a sound numerical basis for the common practice where the incompressible case is usually employed for reservoir simulation tests.

Cases	1a	1b	2a	2b	3a	3b
compressible	709.0	932.5	929.2	1214.7	1079.8	1380.7
incompressible	727.8	950.7	979.8	1243.0	1153.0	1443.0

Table 7. The cumulative oil rates in compressible and incompressible cases.

6. Concluding Remarks

In this paper we have presented a comparison of numerical results obtained using our reservoir simulator with those by fourteen organizations for a benchmark problem. This problem deals with the effect of varying the rate and length of a horizontal well on oil recovery from a reservoir where coning is important. All the simulators have consistently predicted an increase in oil production and a decrease in coning effects with an increase in well length. The comparison with these organizations has also shown that our simulator is correct and reliable. Finally, a comparison between compressible and incompressible cases for the model problem considered has indicated that the latter is a reasonable approximation of the former. This gives us some confidence when the incompressible case is used for numerical simulation tests.

Cases	1a	1b	2a	2b	3a	3b
compressible	3463.55	3586.66	3230.98	3484.47	2991.40	3393.62
incompressible	3513.61	3586.44	3389.43	3529.90	3270.0	3472.0

Table 8. The bottom hole pressure in compressible and incompressible cases.

References

- [1] K. Aziz and A. Settari, *Petroleum Reservoir Simulation*, London, Applied Science, 1979.
- [2] Z. Chen, Formulations and numerical methods for the black-oil model in porous media, *SIAM J. Numer. Anal.* **38** (2000), 489–514.
- [3] L. X. Nghiem, D. A. Collins, and R. Sharma, Seventh SPE comparative solution project: Modeling of horizontal wells in reservoir simulation, SPE 21221, 11th SPE Symposium on Reservoir Simulation in Anaheim, California, Feb. 17-20, 1991.
- [4] D. W. Peaceman, Presentation of a horizontal well in numerical reservoir simulation, SPE 21217, presented at 11th SPE Symposium on Reservoir Simulation in Anaheim, California, Feb. 17-20, 1991.
- [5] T. Russell and M. Wheeler, Finite element and finite difference methods for continuous flows in porous media, Chapter II, *The Mathematics of Reservoir Simulation*, R. Ewing, ed., *Frontiers in Applied Mathematics 1*, Society for Industrial and Applied Mathematics, Philadelphia, **1** (1983), 35–106.
- [6] H. L. Stone, Probability model for estimating three-phase relative permeability, *JPT* **22** (1970), 214–218.

Department of Mathematics, Box 750156, Southern Methodist University, Dallas, TX 75275-0156, USA

E-mail: zchen@mail.smu.edu

URL: <http://faculty.smu.edu/zchen>

Department of Mathematics, Box 750156, Southern Methodist University, Dallas, TX 75275-0156, USA

E-mail: ghuan@mail.smu.edu and bli@mail.smu.edu